

## Gap estimation method between calandria tube and liquid injection nozzle in CANDU reactor

103-16

(sagging)

가

beam

beam

1

### Summary

As the calandria tube(made of zirconium alloy) is sagging due to its thermal and irradiation creep during the plant operation, it possibly contacts with liquid injection nozzle crossing beneath the calandria tube, which subsequently results in difficulties on the safe operation. It is therefore necessary to check the gap for the confirmation of no contacts between the two tubes, calandria tube and liquid injection tube, with a proper measure during the life of plant. In this study, a methodology to estimate the gap between the two tubes utilizing the classical beam theory is proposed. The saggings of the calandria tube and liquid injection tube are modelled as mathematical deflection curves, the coefficient of which is determined by sagging data measured at viewing port by an ultrasonic measurement device. The proposed method was found to be well fitted to some measured data, which means that the method can be applied to Wolsung-1 for the measurement of the gap between calandria tube and liquid injection tube.

1.

( )가 ( pressure  
tube: PT) (calandria tube: CT) CT  
1 , 1 .  
CT  
(sagging) [1,2],  
(liquid injection nozzle; LIN) ( 1 )  
가 .  
CT  
LIN HFD(horizontal flux detector: HFD)  
Bruce A 4 1993 LIN probe  
[3], Pt. Lepreau HFD probe  
CT HFD [4], CT LIN  
가 .  
1 CT LIN 가  
Bruce A 가  
(VP) [5].  
(VP) 1 ( 1  
) 가 CT LIN  
CT LIN  
[6]. probe  
data VP  
1 380 CT가 11.25" , CT LIN 1  
CT F G , Q R 3 ( )  
, 1 ) 6 가  
LIN F /Q CT G /R CT  
. CT CT 가  
, 가  
, CT LIN 가 가 LIN-2 LIN-5  
가 .  
VP 1 VP-1 CT 2 3 ,  
(A ) 80cm가 VP-2 CT 16 17  
, (C ) 60cm 가  
VP 2 3 , 16 17 CT LIN-2 LIN-5가 ,  
CT LIN LIN CT(F3, F16, F17, Q2, Q3, Q16, Q17)

CT (G2, G3, G16, G17, R3, R16, R17)

가  
CT LIN  
beam

가

가

CT LIN

## 2. CT

CT  
calandria tube sheet( 1

CT beam theory  
"A" "C" side )

[7]. CT

2

4

$$y = a_0 + a_1x + a_2x^2 + a_3x^3 + a_4x^4 \quad (1)$$

i) at  $x = 0, y = 0$  (2)

ii) at  $x = 0, \theta = \frac{dy}{dx} = 0$

iii) at  $x = l, y = 0$

iv) at  $x = l, \theta = \frac{dy}{dx} = 0$

$$a_0 = 0, \quad a_1 = 0, \quad a_3 = -\frac{2a_2}{l}, \quad a_4 = \frac{a_2}{l^2} \quad (3)$$

$$y = a_2x^2 - \frac{2a_2}{l}x^3 + a_2\frac{x^4}{l^2} = a_2x^2\left(1 - \frac{x}{l}\right)^2 \quad (4)$$

(4) ( $x = x_i$ )  $y_i$   $a_2$

,  $\delta_{\max}(x = 0.5l)$  ) 가

$$\delta_{\max} = \frac{1}{16} a_2 l^2 \quad (5)$$

### 3. LIN

1 LIN 1 "D" side "B" side  
 locator bracket 3 LIN  
 beam theory CT  
 LIN "D" side  
 "B" side locator bracket 4  
 CT LIN gap  
 LIN  
 beam  
 CT LIN CT LIN  
 , LIN CT CT  
 CT LIN 4 CT  
 ' - ' ( $\Delta_2$ ) ' - ' ( $\Delta_1$ )  
 $\Delta_2 \leq \Delta_1$   
 LIN CT LIN  
 1 LIN ' - ' CT  
 (4) LIN ' - ' 가 CT

### 4. CT/LIN

1 CT LIN  
 LIN-2 CT (F3 F20)  
 LIN-2 CT (G2 G21)  
 LIN-5 CT (Q2 Q21)  
 LIN-5 CT (R3 R20)  
 (VP) 가  
 VP-1: LIN-2 F3 G2, G3  
 VP-1: LIN-5 Q2, Q3 R3  
 VP-2: LIN-2 F16, F17 G16, G17  
 VP-2: LIN-5 Q16, Q,17 R16, R17  
 VP CT  
 가 CT LIN  
 VP-1: G2 Q2, E3 S3  
 VP-2: B16 V16, B17 V17  
 VP CT LIN

( 5 ).

$$A_1 = A_0 - (\delta_{CT} - \delta_{LIN}) \quad (6)$$

$$A_2 = A_0 + (\delta'_{CT} - \delta_{LIN}) \quad (7)$$

CT CT 가 ( ,  $\delta_{CT}$   
 $= \delta'_{CT}$ ),  $A_0$  / CT .

$$A_0 = \frac{A_1 + A_2}{2} \quad (8)$$

VP CT LIN 6  
 . , VP 가 CT LIN  
 CT LIN CT ( $\delta_{CT}$ ) LIN ( $\delta_{LIN}$ )  
 . VP ( 1  $x = x_i$ ) CT ( $\delta_{CT}$ ) (4)  
 . LIN CT

LIN  
 LIN LIN  
 CT LIN  
 CT 가 ( )  
 [1,2] VP 가 CT  
 1 ( 7 ) M, N, O 16 17 CT  
 . CT CT  
 CT LIN .

5.

가 Bruce A [3].  
 Bruce A 4 CT 가 1 480 900MW . 1979  
 1993 CT LIN 14  
 LIN CT (P01 P19) CT (Q01 Q19)  
 2  
 Bruce A 4 VP-2 CT  
 LIN CT 2  
 10% 가 .

6.

(CT)

CT

(LIN)

- (1) CT LIN beam
  - (2) CT LIN
  - (3) CT LIN 가 CT CT
  - (4) LIN 가 (VP-2) CT
- 1 CT LIN

[1] V. Fidleris, "The Irradiation Creep and Growth Phenomena," J. of Nuclear Materials, vol. 159, 1988, pp22-42.

[2] A. R. Causey, F. J. Butcher and S. A. Donahue, "Measurement of Irradiation Creep of Zirconium Alloys Using Stress Relaxation," J. of Nuclear Materials, vol. 159, 1988, pp101-113.

[3] R. C. Abucay, K. S. Mahil and J. Goszczynski, "Recent Experience in Ultrasonic Gap Measurement between Calandria Tubes and Liquid Injection Shutdown System Nozzle in Bruce Nuclear Generating Station," Proc. of 13th Int. Conf. on NDE in the Nuclear and Pressure Vessel Industry, Kyoto, Japan, 1995.5

[4] J. Goszczynski and A. B. Mitchell, "Development of Ultrasonic Measurement of Calandria Tubes/Horizontal Flux Monitor Guide Tube Proximity in CANDU Nuclear Reactors,"

[5] , , , , 1 , , , 1999.6

[6] , , , , " , 2000 , 2000. 5. 26-27,

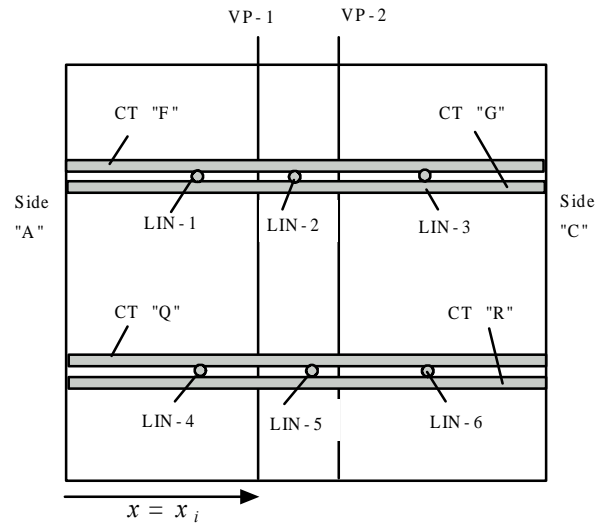
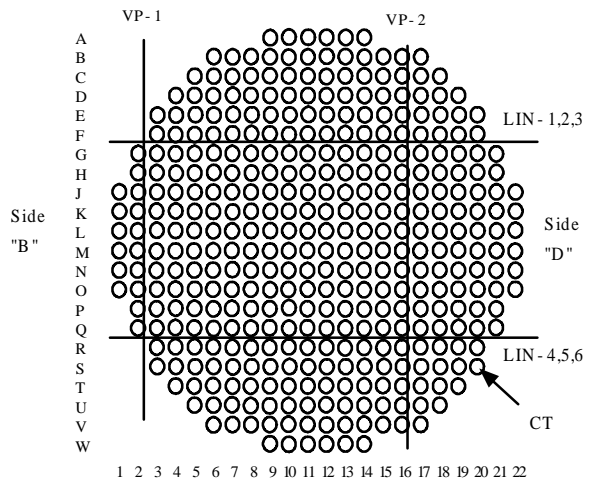
[7] R. J. Roark and W. C. Young, Formulas for Stress and Strain, 5th ed. McGraw-Hill 1975.

1 1

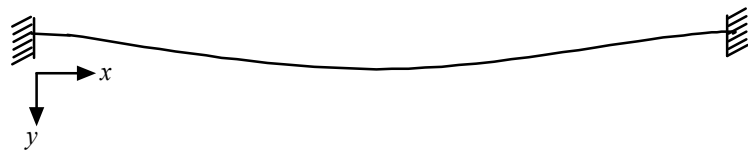
		(mm)	(mm)	(mm)	
PT	380	A: 6185.6 B: 6170.4 C: 6155.2	104.8	4.19	Zr 2.5% - Nb
CT	380	5944	128.96	1.37	Zircaloy - 2
LIN	6	7320	50.8	2.79	Zircaloy - 2
HFD	7	12530	2.73/ 1.65/ 0.34	6.22/ 0.50/ 0.2	Zircaloy - 2/ SS/ Al
VFD	26	14300	3.04/ 2.20/ 0.34	7.11/ 1.65/ 0.2	Zircaloy - 2/ SS/ Al

2 (VP-2 ) (Bruce A 4 )

	P ( ) gap			Q ( ) gap		
			(%)			(%)
P01/ Q01	23.92	18.04	- 24.6	59.52	65.40	9.9
P02/ Q02	21.87	19.25	- 12.0	61.57	64.19	4.3
P03/ Q03	22.55	21.31	- 5.5	62.26	63.51	2.0
P04/ Q04	23.92	22.05	- 7.8	59.52	61.39	3.1
P05/ Q05	23.92	24.53	2.6	61.57	60.97	- 1.0
P06/ Q06	23.92	25.58	6.9	60.89	59.24	- 2.7
P07/ Q07	25.97	26.53	2.2	58.16	57.61	- 0.9
P08/ Q08	25.28	27.66	9.4	58.84	56.46	- 4.0
P09/ Q09	28.02	29.31	4.6	57.47	56.19	- 2.2
P10/ Q10	28.71	30.40	5.9	57.47	55.78	- 2.9
P11/ Q11	29.39	29.55	0.5	54.06	53.91	- 0.3
P12/ Q12	29.39	29.80	1.4	54.06	53.66	- 0.7
P13/ Q13	30.76	30.83	0.2	54.75	54.69	- 0.1
P14/ Q14	30.76	30.92	0.5	55.43	55.28	- 0.3
P15/ Q15	28.71	29.04	1.1	54.75	54.42	- 0.6
P16/ Q16	28.71	27.95	- 2.6	54.06	54.83	1.4
P17/ Q17	29.39	29.38	0.0	58.16	58.18	0.0
P18/ Q18	28.02	28.92	3.2	60.89	60.00	- 1.5
P19/ Q19	23.24	23.87	2.7	58.16	57.53	- 1.1

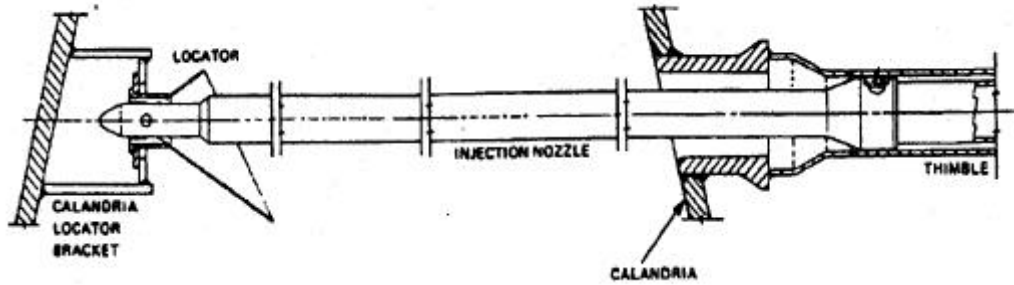


1 1 ( )



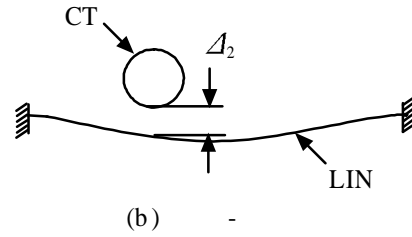
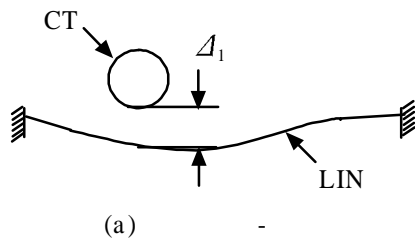
2 CT





3 LIN

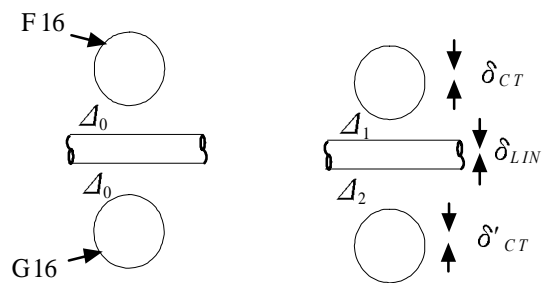
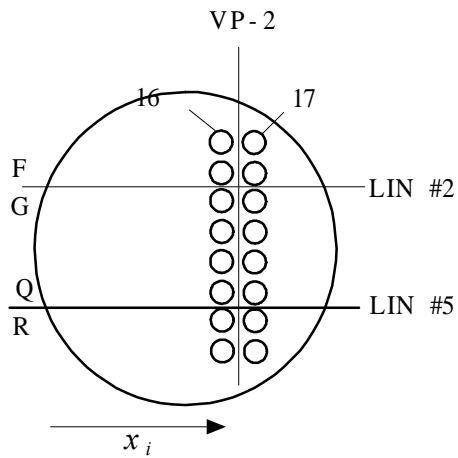
support



4

LIN

CT



$\Delta_0$  : gap

$\Delta_1$  : CT LIN gap

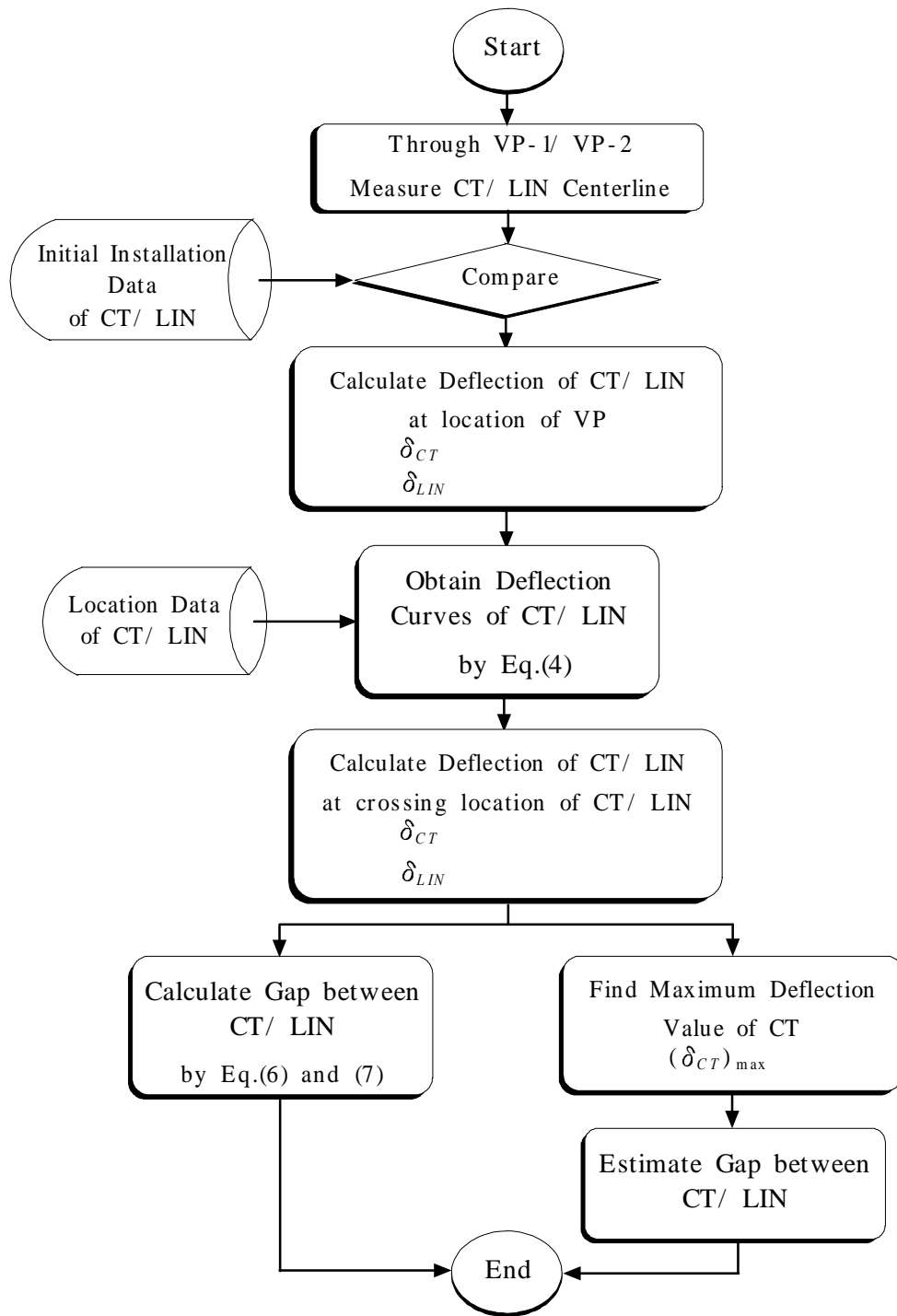
$\Delta_2$  : CT LIN gap

$\delta_{CT}$  : CT

$\delta'_{CT}$  : CT

$\delta_{LIN}$  : LIN

5 CT/LIN



	VP1															VP2											
	1	2	3	4	5	6	7	8	9	10	11	12	13	14	15	16	17	18	19	20	21	22					
A									325	338	346	348	341	351									A				
B							282	348	397	425	445	450	452	450	433	405	353	297					B				
C						326	366	447	493	523	530	536	530	544	531	502	456	393	331				C				
HFDB/D						342	408	475	532	571	594	602	594	596	608	602	581	542	483	413	343		D				
E						331	412	481	541	587	615	626	628	619	621	634	635	624	598	547	484	412	328				
UH/BS						401	480	538	585	618	634	629	627	621	623	632	636	642	629	590	539	477	366				
G						367	457	534	575	610	633	643	635	634	635	637	639	642	649	636	611	572	528	448	357		
HF/D1						417	509	578	605	623	643	648	642	642	645	646	646	647	653	646	627	599	569	497	405		
J						339	451	547	610	622	635	643	647	645	644	645	646	648	649	650	644	631	614	597	532	436	326
HF/D2						362	481	576	632	632	639	647	649	646	644	639	641	647	650	651	649	633	622	618	559	464	347
L						377	496	591	649	653	655	654	652	649	642	632	634	645	651	654	654	650	642	633	573	478	361
HF/D3						374	495	592	652	650	653	650	655	649	643	632	633	646	653	656	650	659	651	638	575	479	360
M						356	476	577	642	658	665	660	655	650	645	637	639	649	655	660	665	663	652	630	562	463	343
HFDB/9						333	448	549	619	649	663	658	655	650	648	649	651	653	656	662	663	664	646	611	538	437	322
P						410	503	576	610	636	650	654	646	647	652	654	652	654	663	657	640	609	572	496	402		
UH/BS						358	445	521	562	600	628	641	637	640	645	640	647	647	652	636	607	565	520	441	352		
R						389	456	507	559	602	627	630	635	635	638	643	642	640	619	588	513	459	382				
S						310	384	445	509	567	605	626	634	627	630	643	636	620	582	520	454	389	312				
T						309	372	440	503	549	578	591	585	589	600	591	564	518	453	382	315						
U						288	349	413	464	498	517	516	519	525	510	477	427	361	298								
V						245	304	357	390	413	421	423	419	399	367	319	255										
W																											